UCRL-TR-237310

LAWRENCE
LIVERMORE
NATIONAL
LABORATORY

NRL FTF 0.5MJ-Class Nominal Baseline Target

K. N. LaFortune, L. J. Perkins

December 17, 2007

Disclaimer

This document was prepared as an account of work sponsored by an agency of the United States government. Neither the United States government nor Lawrence Livermore National Security, LLC, nor any of their employees makes any warranty, expressed or implied, or assumes any legal liability or responsibility for the accuracy, completeness, or usefulness of any information, apparatus, product, or process disclosed, or represents that its use would not infringe privately owned rights. Reference herein to any specific commercial product, process, or service by trade name, trademark, manufacturer, or otherwise does not necessarily constitute or imply its endorsement, recommendation, or favoring by the United States government or Lawrence Livermore National Security, LLC. The views and opinions of authors expressed herein do not necessarily state or reflect those of the United States government or Lawrence Livermore National Security, LLC, and shall not be used for advertising or product endorsement purposes.

NRL FTF 0.5MJ-Class Nominal Baseline Target
Hydra 1D/2D Results – Dec. 10, 2007

Kai N. LaFortune, L. John Perkins
(in collaboration with Andy Schmitt from NRL)

Summary:
This memo summarizes the latest progress in work on NRL 0.5 MJ-class FTF target.
Since the last discussion, 1D performance issues have been resolved. The 1D
performance issues inadvertently resulted from an effort to carefully compare the Lasnex
and Hydra target simulations. The work has been expanded to 2D simulations of linear,
single-l-mode growth simulations. The 2D simulations of mode growth in the linear
regime indicate the target has a peak mode growth of around 1500x occurring near $l=125$.

1D performance summary:
In the fall of '06, the two LLNL simulations disagreed modestly in performance: the
Hydra simulations giving anomalously higher yields than Lasnex or even the FAST
simulations. The input decks for both simulations were carefully reviewed. In the
process of doing so, the simulations were stripped of complexities that may have
introduced differences in target performance due to subtleties in the differences in which
the physics was implemented in the two models. This included changing the EOS model
from an older QEOS model to a more relevant, less-compressible, tabular LEOS model
(see previous memo for details). It also included changing several input parameters and
simplifying the radiation transport binning. In the spring of '07, the LLNL team had
targets that did not burn unless the drive energy was dramatically increased (>60%).
Initially, this increase was erroneously attributed to the newer, less-compressible EOS
model. Subsequent perusal of the older, working decks and comparison with the recent
decks revealed that the final state of the radiation transport model was oversimplified.
The initial models had the radiation spectrum divided up into 90 bins. In intermediate
cases the radiation transport was turned off completely. When the radiation transport was
turned back on, one bin was used (i.e., the radiation spectrum was assumed to be
Planckian). This is why the target simulations stopped working. The multi-group
radiation diffusion model has been re-implemented; although, 90 bins are more than are
needed to accurately keep track of the radiation diffusion.

Target specs:

Initial temp: 1e-6 keV

Initial geometry:

Region	At. fracts	Density(g/cc)	Radius (cm)	Thickness
DT gas	1:1	2e-4	0.0852	0.0852
DT fuel	1:1	0.2564	0.1058	0.0206
CHDT Abl	1:1:5.94:5.94	0.3312 (100mg/cc foam)	0.1189	0.0131
CH shell	1:1	1.070	0.1194	0.0005

We employ a foam ablator density of 100mg/cc (GA recommended minimum density for practical fabrication); a 40 mg/cc foam ablator similar to that of NRL was also run but the results will not be discussed here except to mention that there were no surprises in the performance. The only other small difference was DT ice density of 0.2564 vs. 0.2500.

EOS model:

For the DT gas and ice layers the EOS of choice was the LEOS table #1018 (same as NIF), which is the one benchmarked to Sandia and Russian data (see March '07 memo for references). It is less compressible than original QEOS model used. This is not the cause, as previously thought, of the decrease in the robustness of the 0.5 MJ target simulations. The choice of EOS for the ablator layer was less obvious. Hydra currently does not support mixing tabular LEOSes within a region. And, there is no LEOS table for 100 mg/cc or 40 mg/cc wicked DT CH foam. Therefore, the choices are to stick with the older QEOS model that we know to be somewhat more compressible or to use the LEOS table for DT in the ablator. For the results in this memo, we have chosen to use the older QEOS model.

Critical Hydra Parameters:
Over the course of the past year, an effort was made to minimize discrepancies between Hydra and the other models (LASNEX & FAST) not just in the geometry of the source and target but also in the various parameters passed to the models. A careful audit of the parameters used uncovered some discrepancies. Below is a list of critical parameters that were discussed and their latest values in the Hydra simulations.

Parameter	Value	Comment
rflxm	1.e20	Radiation flux limiter: equivalent to Perkins' value of 0. This value essentially turns off radiation flux limiter; a setting of 0 would inhibit all radiation flux
eflxm	1.272/.10	Electron flux limiter: equivalent to NRL's value for the electron flux
iflaser	3	Spherical source (purely radial rays)
rncrs	1.4e-18 (for all regions)	Regional neutron scattering cross section

1D results:

With the proper parameters, EOS model and radiation transport granularity, it was easy to achieve target performance similar to that achieved in the NRL point design. The laser pulse shape, after shock timing, appears in Figure 1. Note: we are still using a spherically-symmetric source, so all rays are radially-incident, there is no laser imprint (for 2D) and there is no "zooming" of the focal spot.

Integral values:

```
drive energy           = 0.449 MJ
absorbed energy        = 0.446 MJ
yield                  = 31.2510 MJ
gain                   = 69.658 MJ
peak fuel velocity     = 3.861e+07 cm/sec
at time                = 8.39 ns
fuel entropy @ peak    = 6.868e+08 J/gm/keV
Vfuel⁷·⁹ /sument⁹·⁵    = 9.67e-25
```

The data presented in this memo continued to use 90 bin multi-group radiation diffusion. But, much effort has gone into optimizing the radiation transport binning granularity for simulation run time. At 90 bins, 90% of the computational cost is in the radiation transport. Figure 5 illustrates the relationship between the material opacity and radiation spectrum (sampled with the full 90 bins). The goal, of course, is to minimize the number of bins without under-sampling the spectral features. Note the features near 0.3-0.4 eV.

2D performance:

With the 1D target shock-timed, 2D simulations of perturbation growth were performed. 2D single mode linear stability analysis was performed by applying a small perturbation (1.0e-9cm amplitude) on outside of ablator, feathered to zero at the fuel-ablator interface. The 5 micron outer shell was conformally mapped onto the outside of the perturbation. The mode amplitude at both the ablation front and the fuel-ablator interface were tracked during these simulations. The simulations ran with low (numerical) noise as measured by comparing the mode shape at time t to the shape at time zero (see examples in Figure 6 and 7 for l=25 and l=125, respectively).

The mode growth as measured by the ratio of the mode amplitude at peak kinetic energy to the amplitude at time zero, is plotted in Figure 8 as a function of l mode number. It peaks around l = 125 after going through a sign reversal between l = 75 & l = 100. The mode amplitude is characterized three different ways: by the mesh perturbation at the ablation front and by the integral rho-R perturbation integrated out to the ablation front and also to the edge of the problem. The location of the ablation front is defined to be the mesh node for which the gradient in density is a maximum. In the figures in the appendix of the time-dependence of the perturbations, the blue curve is the integral up to the ablation front and the cyan curve is the integral over the whole problem. The integral rho-R perturbation up to the ablation front goes through a phase shift but that over the whole problem does not. There does not seem to be a strong dependence on the choice of upper limit of integration. The amplitude of the perturbation measured at intermediate positions goes through a smooth transition from one value to the other.

Appendix (Figures):
(see accompanying documents for additional figures – e.g., plasma radial profiles versus times and a set of time dependent growths for each l-mode)
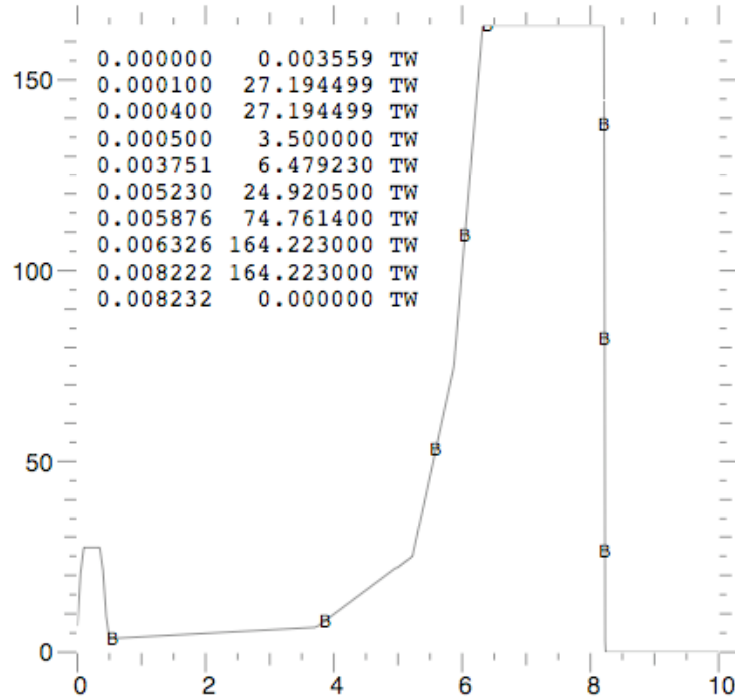


```
        0.000000    0.003559 TW
150 —   0.000100   27.194499 TW
        0.000400   27.194499 TW
        0.000500    3.500000 TW
        0.003751    6.479230 TW
        0.005230   24.920500 TW
        0.005876   74.761400 TW
        0.006326  164.223000 TW
100 —   0.008222  164.223000 TW
        0.008232    0.000000 TW
```

Figure 1: Laser power (in TeraWatts) as a function of time (in nanoseconds) after shock timing.
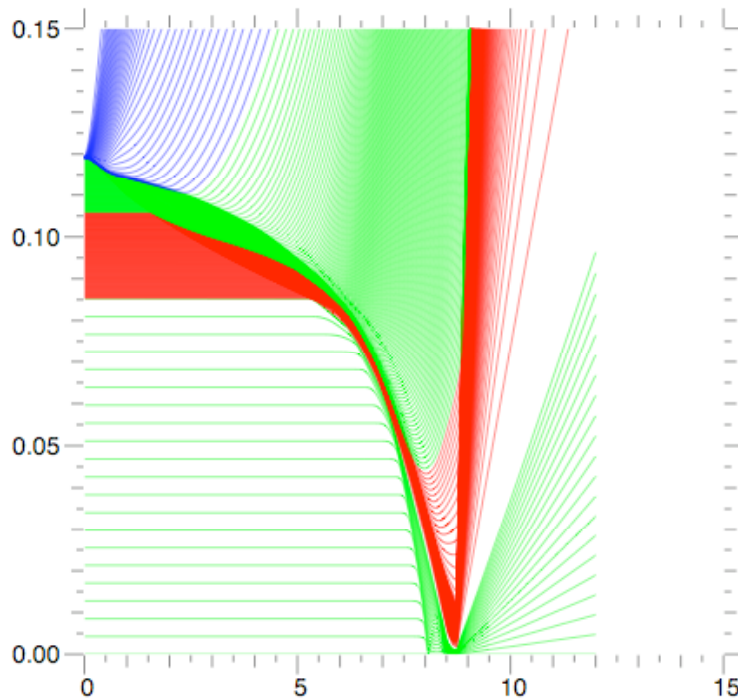
Figure 2: 1D target geometry (cm) as a function of time (ns). yellow = DT gas, red = DT fuel, green = CHDT ablator, blue = CH shell
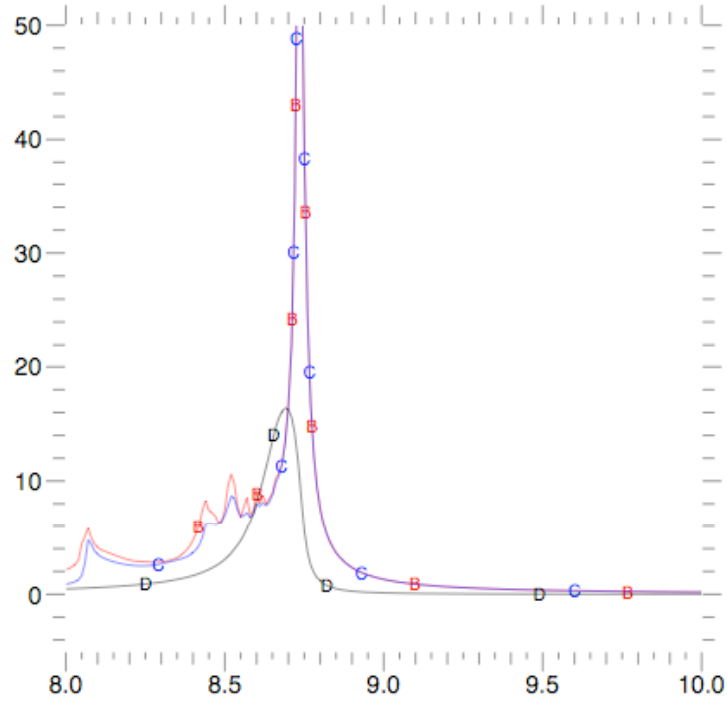
Figure 3: In keV, on-axis ion temp (B) the density-weighted ion temp (C) and the integral rho-R x10 (D), as functions of time (ns). Max rho-R = 1.64 at 8.7 ns and max ion temp = 63 keV.
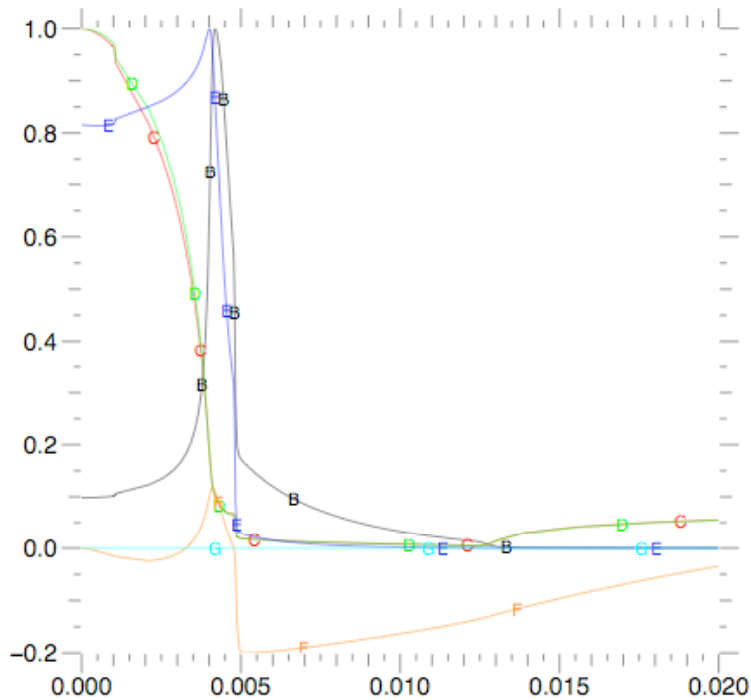
Figure 4 Radial slice at ignition of normalized density (B), ion temp (C), electron temp (D), pressure (E), velocity (F) and integral laser deposition (G) (see accompanying document for details and radial slices at other times).
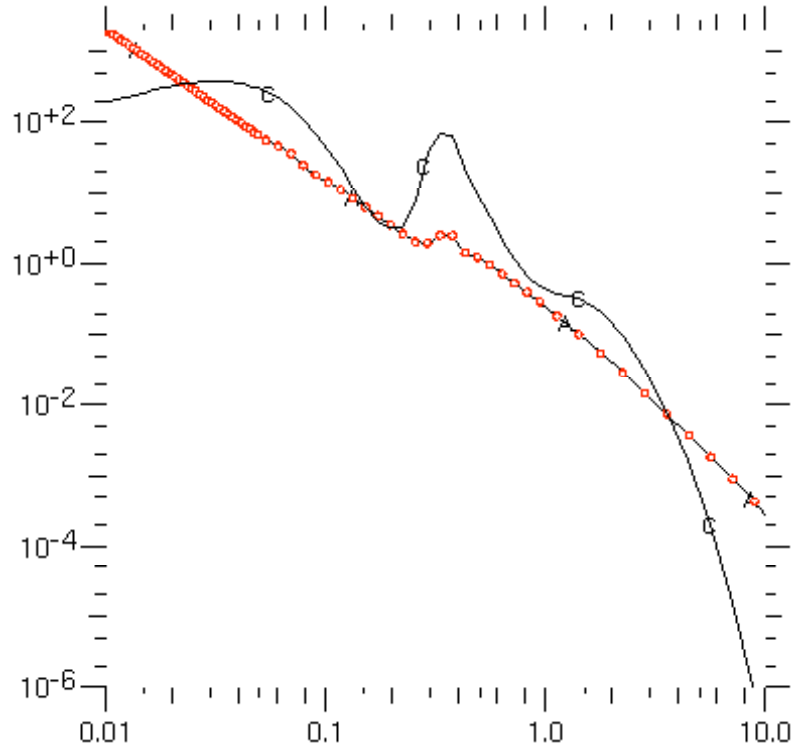
Figure 5: Opacity of DT in target (A, red dot) and radiation density (C) as a function of energy (in keV).
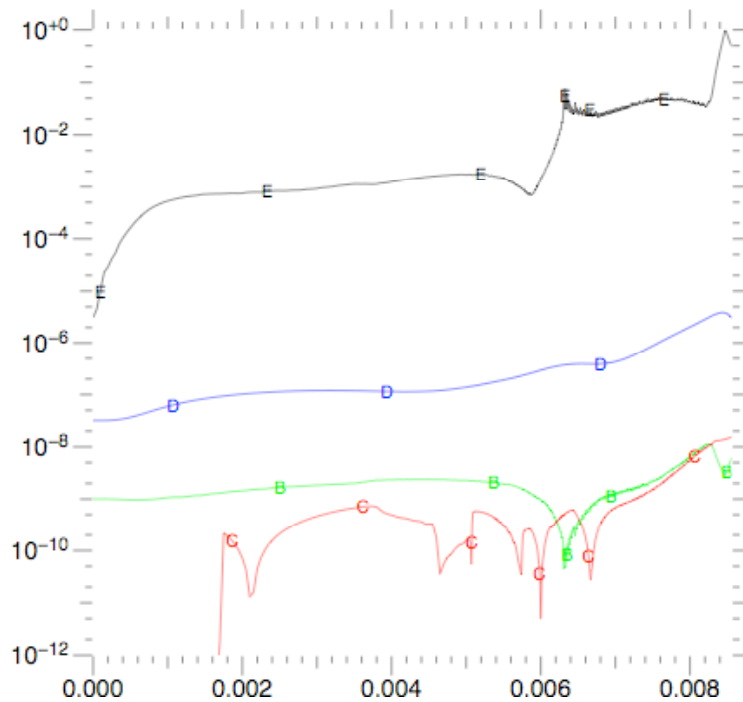
Figure 6 l mode = 25, the peak-to-valley mode aplitude in cm at the ablation front (B) and fuel-ablator interface (C) and the rho-R perturbation (D) as a function of time (in microseconds). Also plotted is the chi-square fit of the mode at the ablation front.

Figure 7: l mode = 125, the peak-to-valley mode amplitude in cm at the ablation front (B) and fuel-ablator interface (C) and the rho-R perturbation (D) as a function of time (in microseconds). Also plotted is the chi-square fit of the mode at the ablation front (E). See accompanying document for figures for other mode numbers.
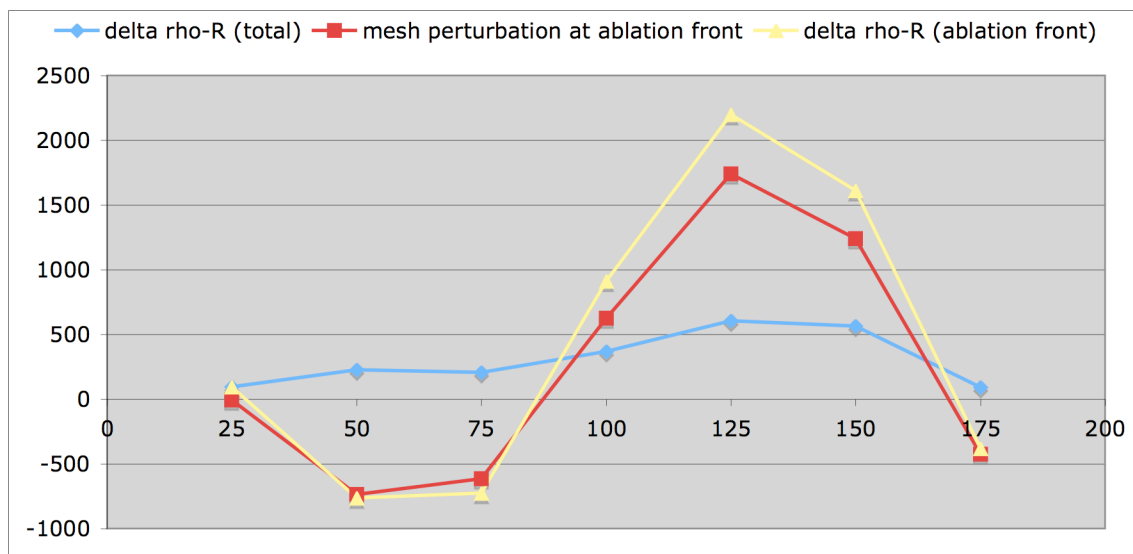
Figure 8: Mode growth factor as a ratio of the amplitude of the mesh perturbation at peak velocity to its amplitude at t=0 ns (red). Note: negative mode growth corresponds to a net phase change. Growth factors of the amplitude of the integral rho-R perturbation with the upper limit of the integral at the ablation front (yellow) and at the edge of the problem (blue).
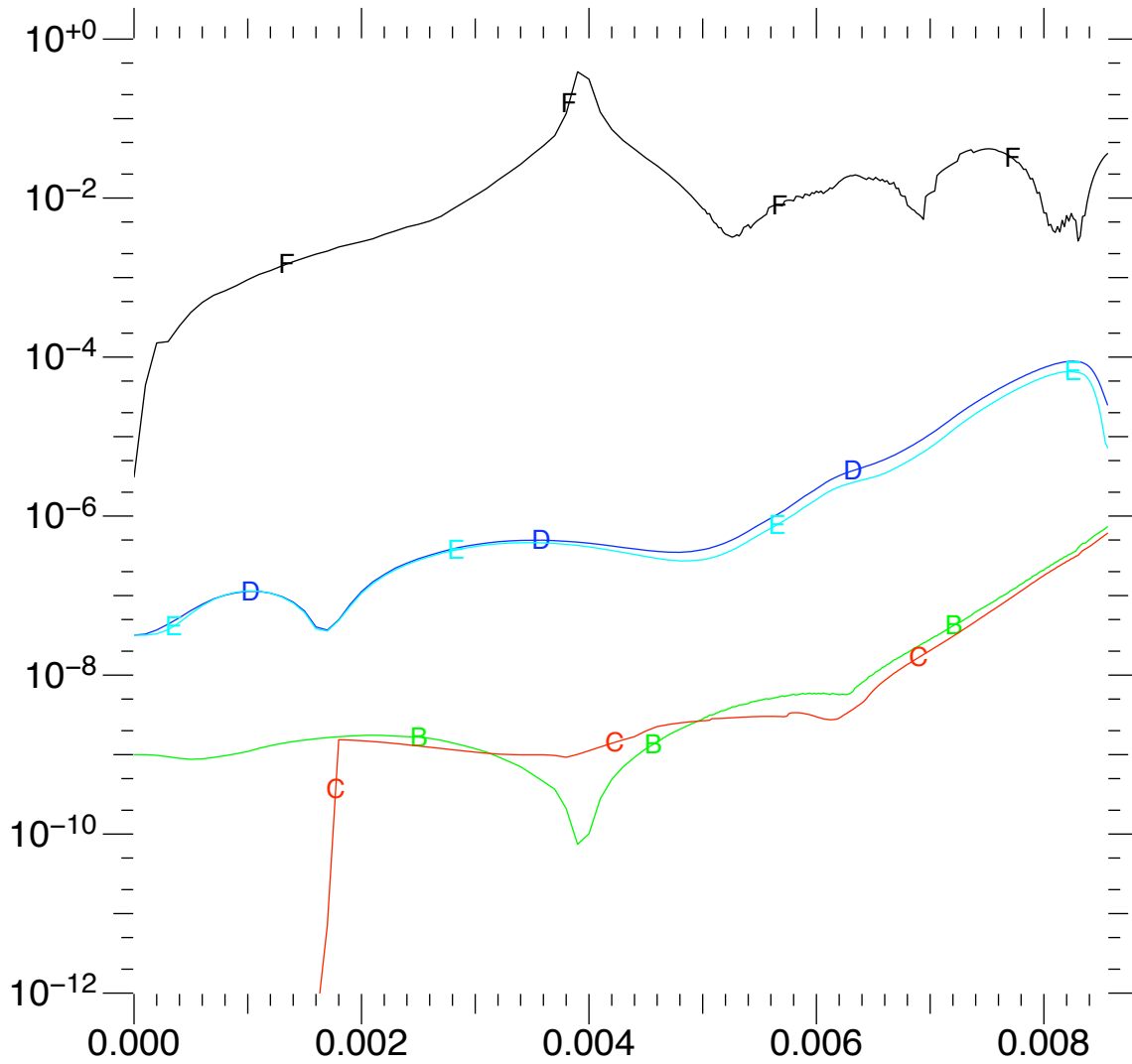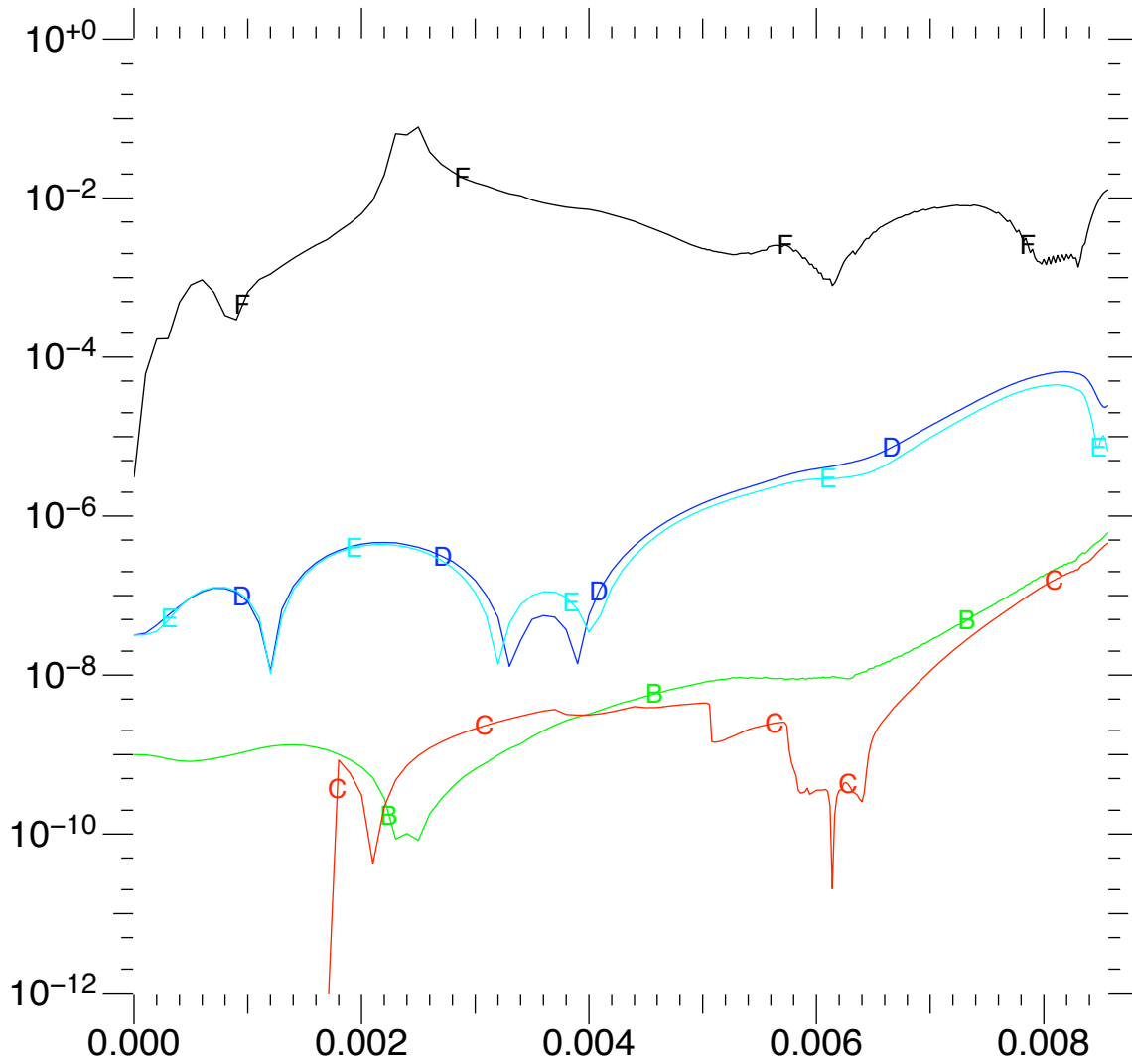
filename = gftf
creation date = 2007−10−09 12:16:33
print date = Thu Dec 13 13:56:08 2007
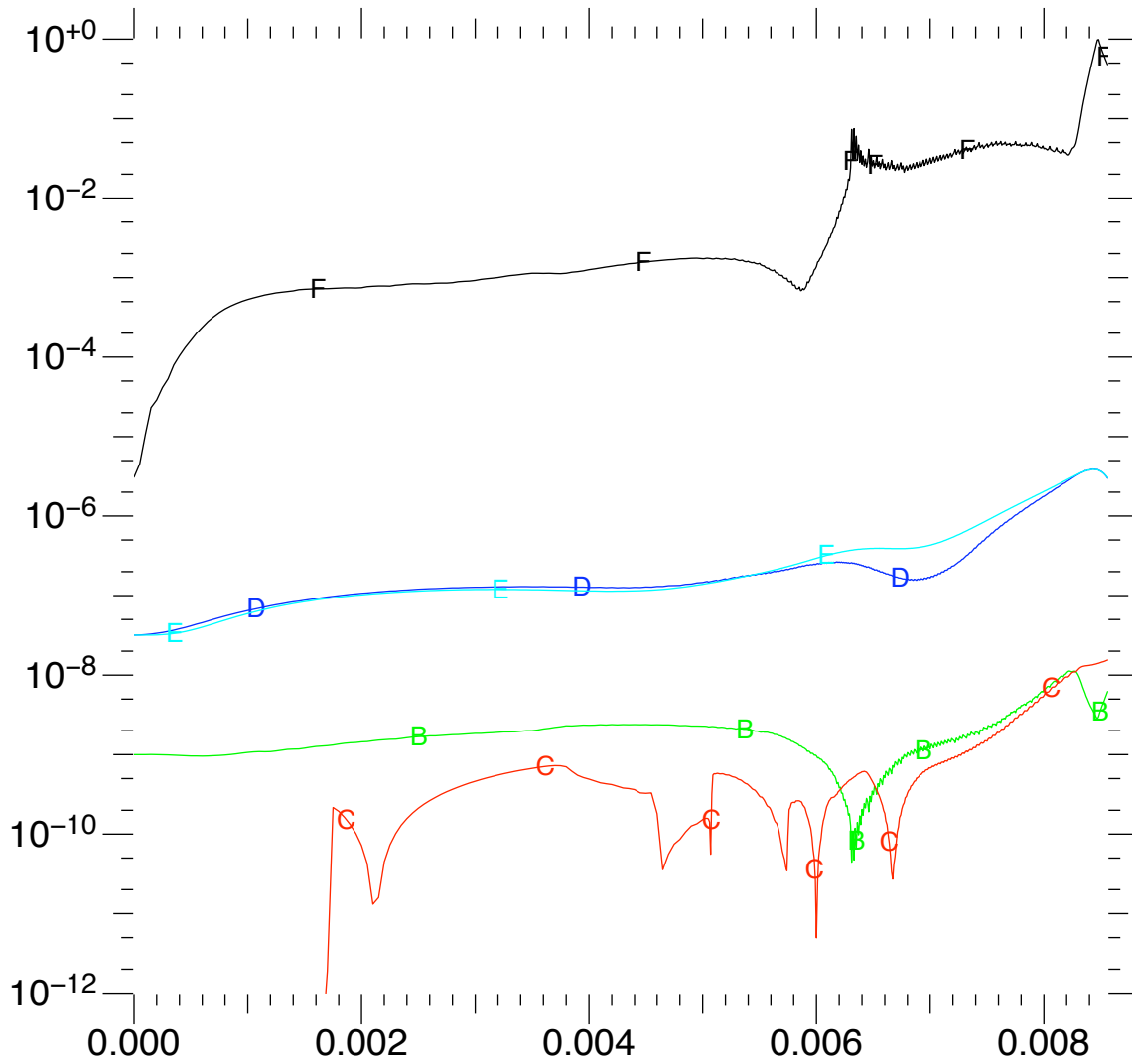
B: plg, abs(mode_amplitude), t
C: plg, fa_amplitude, t
D: plg, rho_r_amplitude, t
E: plg, rho_r_total_amplitude, t
F: plg, chi_squared_fit, t

time of max KE	=	0.00856002
last time step at		0.00892000 microseconds
mode number	=	25
mode growth factor	=	−6.22e+00
rho−R growth factor	=	9.38e+01

B: plg, abs(mode_amplitude), t
C: plg, fa_amplitude, t
D: plg, rho_r_amplitude, t
E: plg, rho_r_total_amplitude, t
F: plg, chi_squared_fit, t

```
time of max KE       =       0.00856001
last time step at            0.00896000 microseconds
mode number          =          50
mode growth factor =       -7.35e+02
rho-R growth factor =       -7.62e+02
```
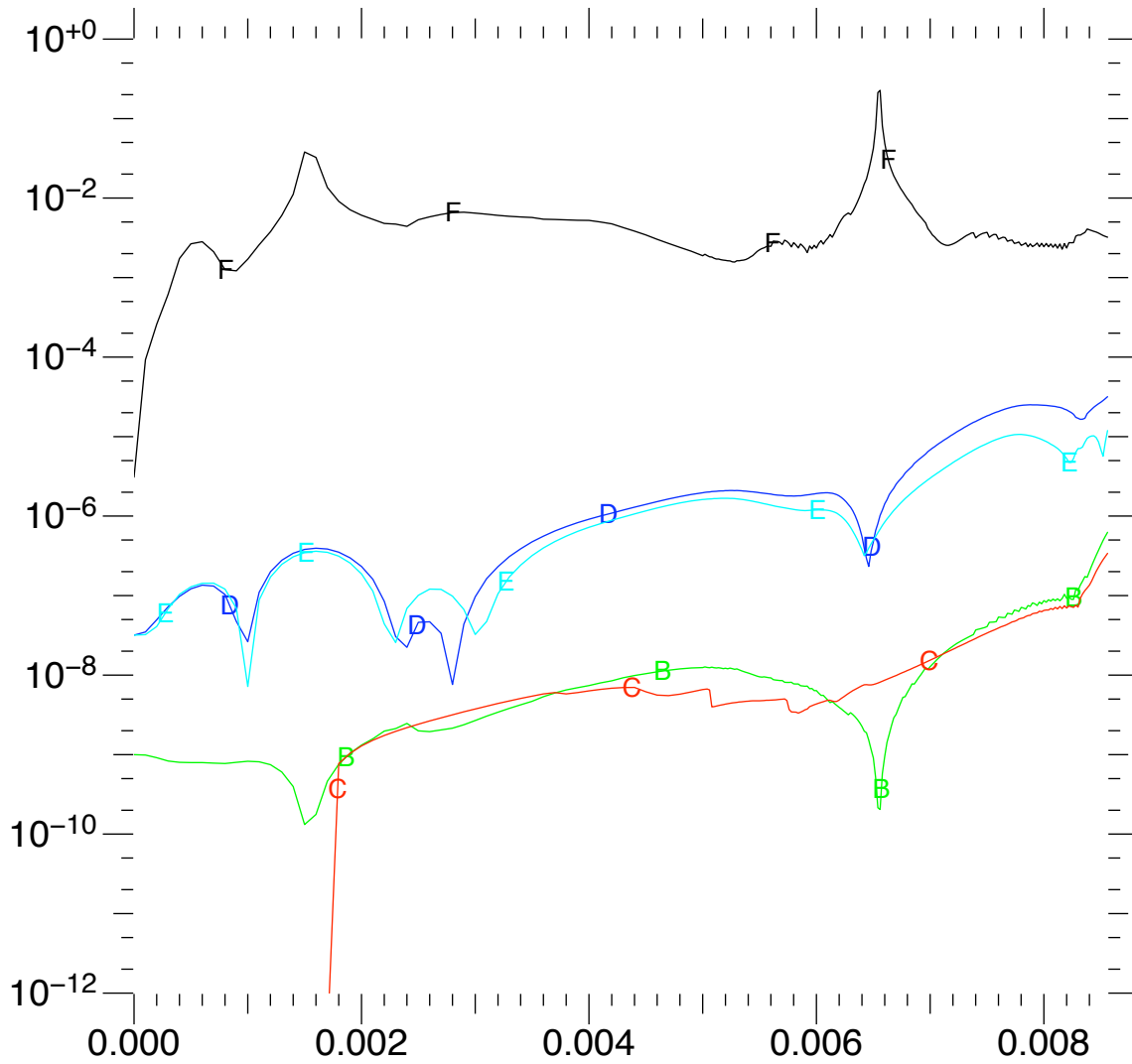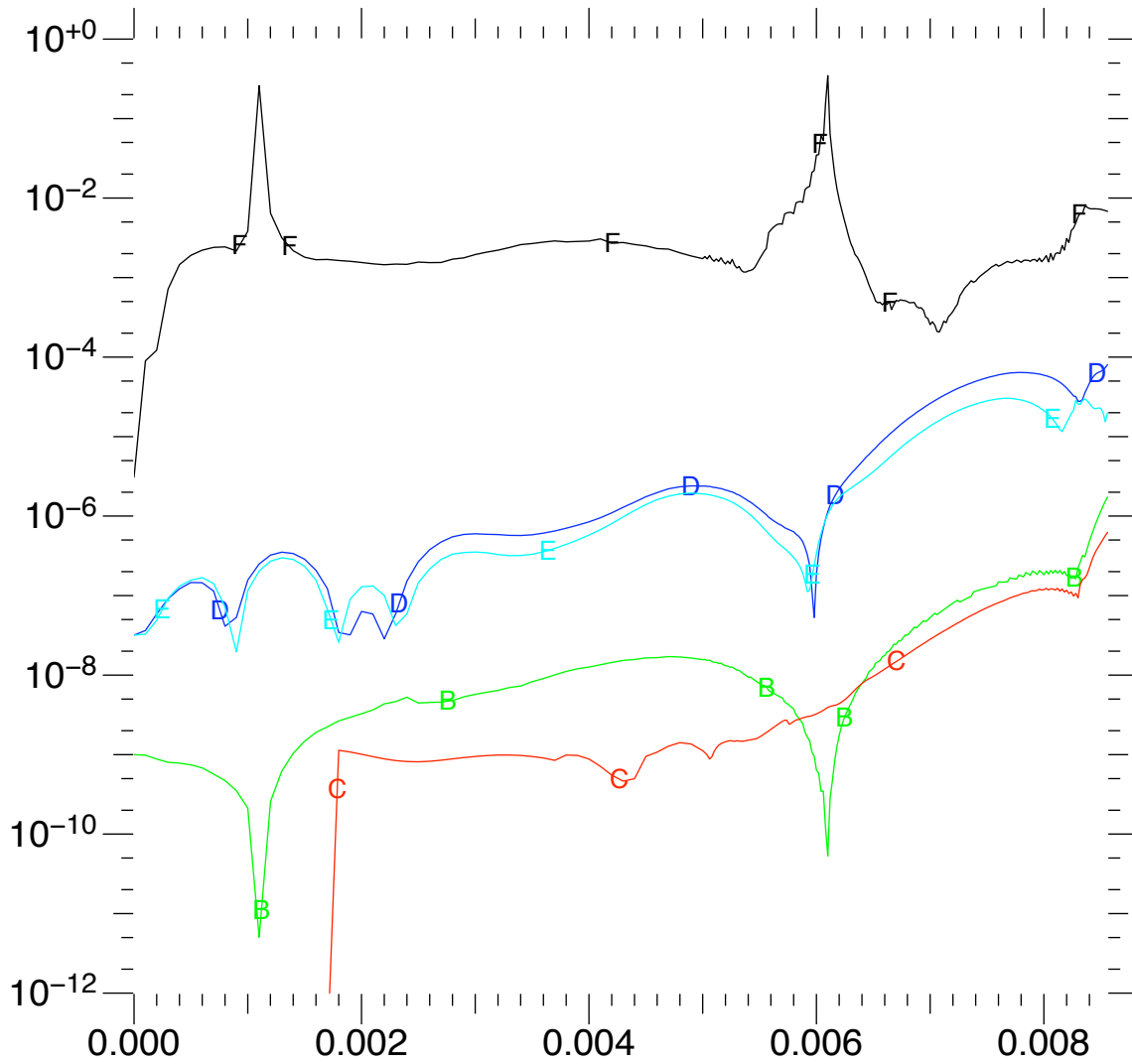
filename = mftf
creation date = 2007−10−18 15:54:18
print date = Thu Dec 13 13:56:37 2007

B: plg, abs(mode_amplitude), t
C: plg, fa_amplitude, t
D: plg, rho_r_amplitude, t
E: plg, rho_r_total_amplitude, t
F: plg, chi_squared_fit, t

time of max KE	=	0.00856001	
last time step at		0.00894000 microseconds	
mode number	=	75	
mode growth factor =		−6.15e+02	
rho-R growth factor =		−7.28e+02	

B: plg, abs(mode_amplitude), t
C: plg, fa_amplitude, t
D: plg, rho_r_amplitude, t
E: plg, rho_r_total_amplitude, t
F: plg, chi_squared_fit, t

```
time of max KE        =        0.00856001
last time step at              0.00892000 microseconds
mode number           =        100
mode growth factor =           6.25e+02
rho−R growth factor =           9.11e+02
```
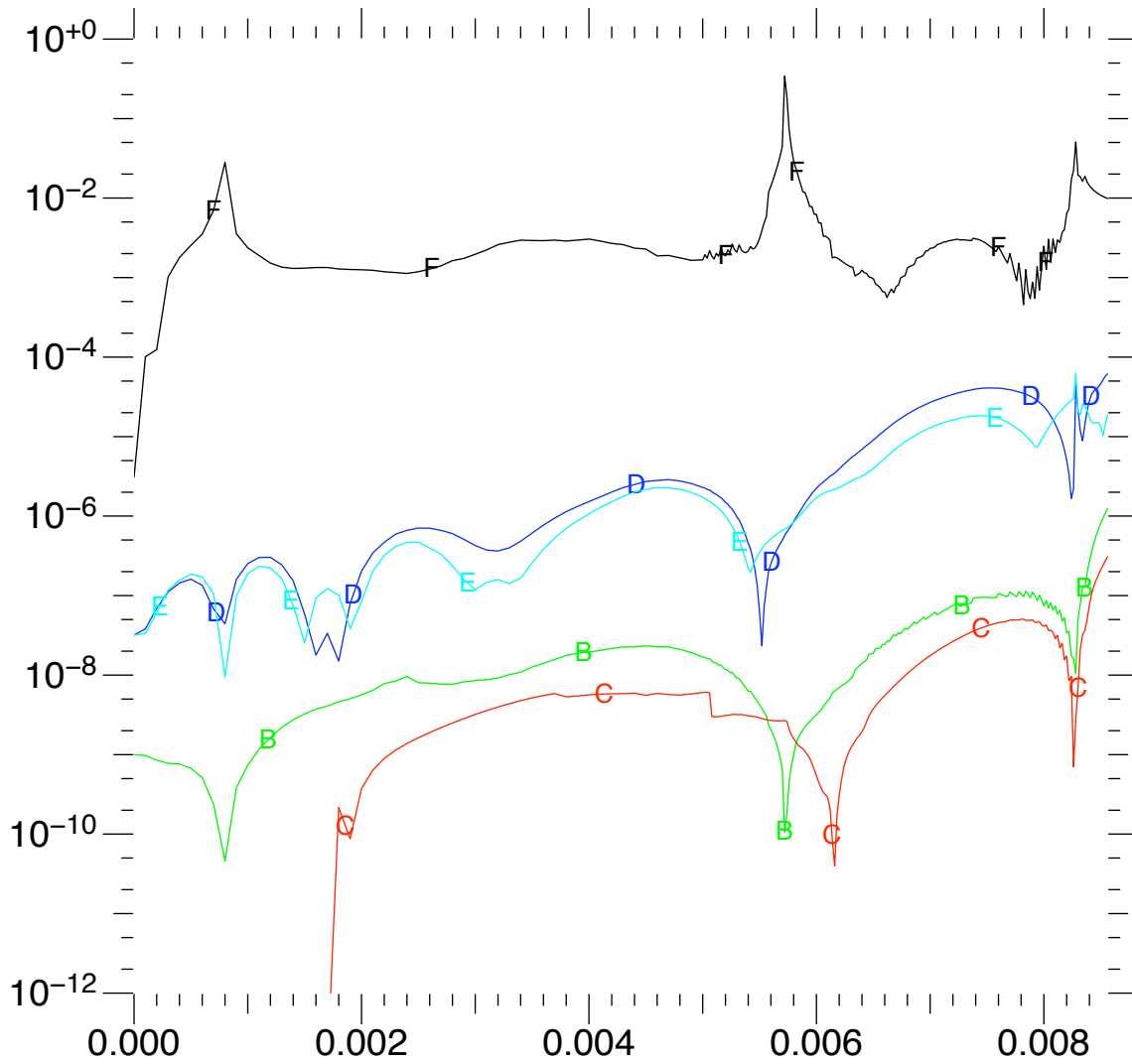
B: plg, abs(mode_amplitude), t
C: plg, fa_amplitude, t
D: plg, rho_r_amplitude, t
E: plg, rho_r_total_amplitude, t
F: plg, chi_squared_fit, t

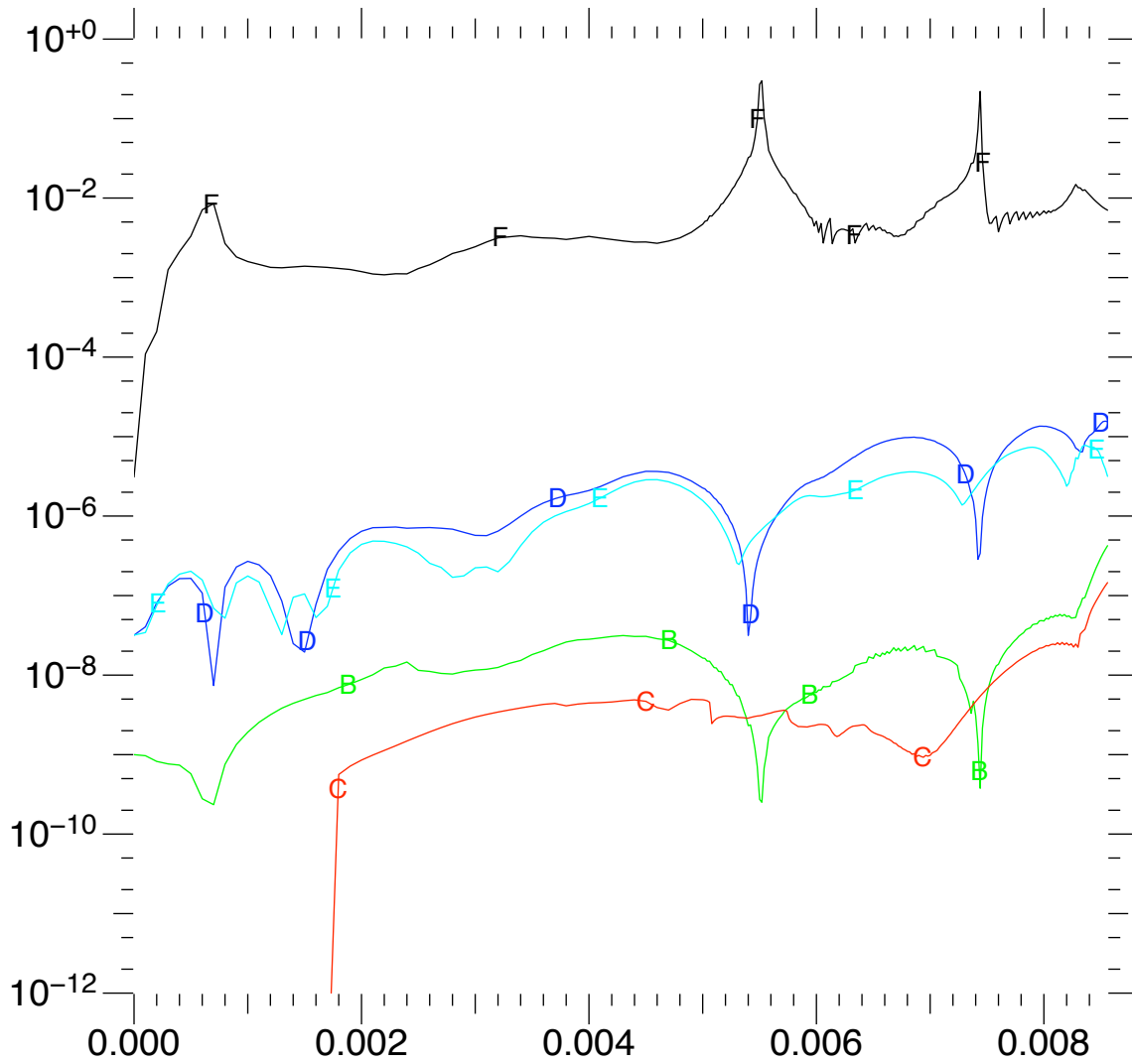|	
time of max KE =	0.00856003
last time step at	0.00886000 microseconds
mode number =	125
mode growth factor =	1.74e+03
rho-R growth factor =	2.20e+03

filename = pftf
creation date = 2007-10-23 14:13:51
print date = Thu Dec 13 13:57:51 2007

B: plg, abs(mode_amplitude), t
C: plg, fa_amplitude, t
D: plg, rho_r_amplitude, t
E: plg, rho_r_total_amplitude, t
F: plg, chi_squared_fit, t

time of max KE   =   0.00856002
last time step at   0.00886000 microseconds
mode number   =   150
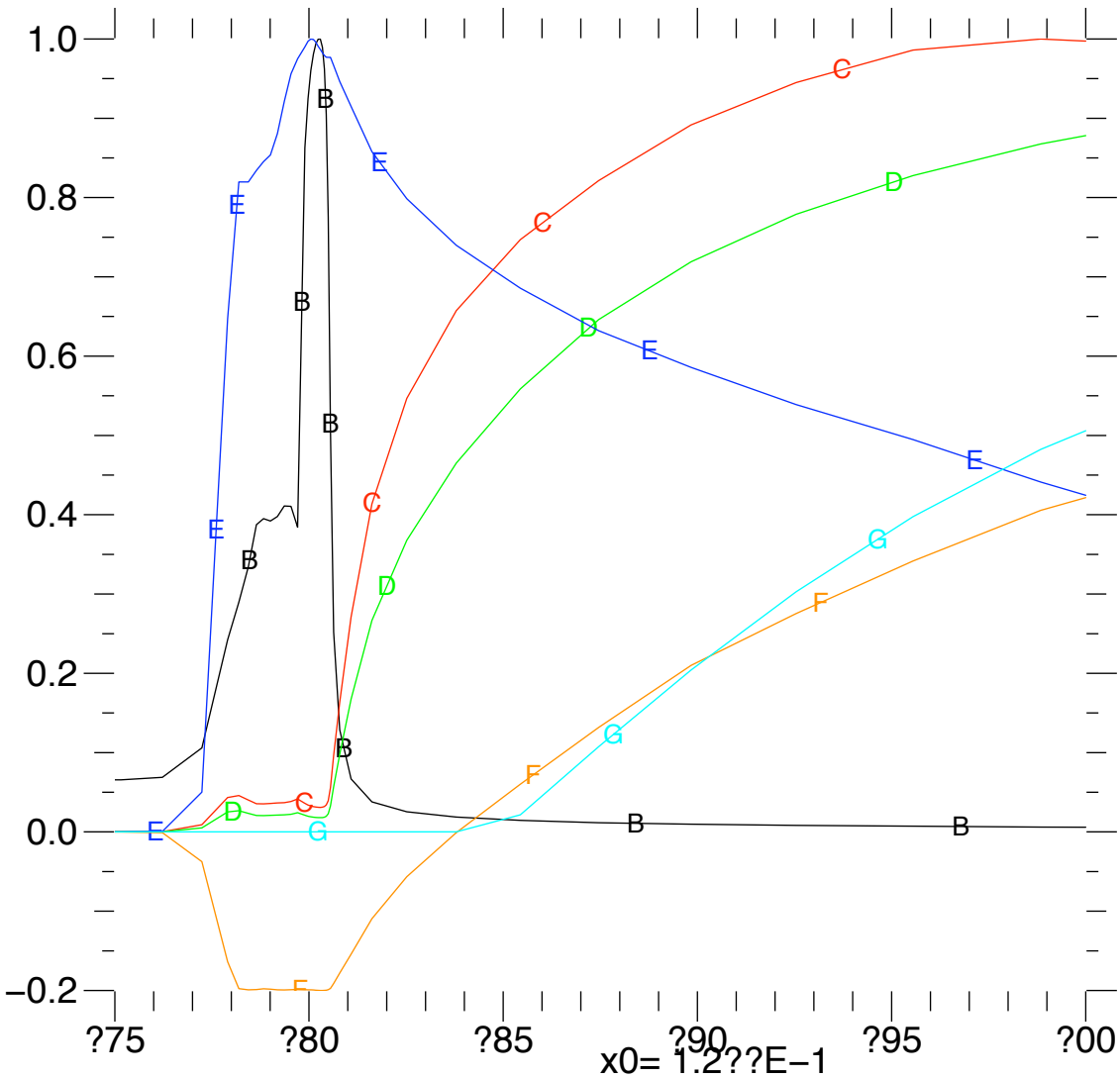mode growth factor =   1.24e+03
rho-R growth factor =   1.61e+03

```
B: plg, abs(mode_amplitude), t
C: plg, fa_amplitude, t
D: plg, rho_r_amplitude, t
E: plg, rho_r_total_amplitude, t
F: plg, chi_squared_fit, t
```

```
time of max KE      =        0.00856002
last time step at            0.00884000 microseconds
mode number         =        175
mode growth factor =         −4.24e+02
rho−R growth factor =         −3.81e+02
```
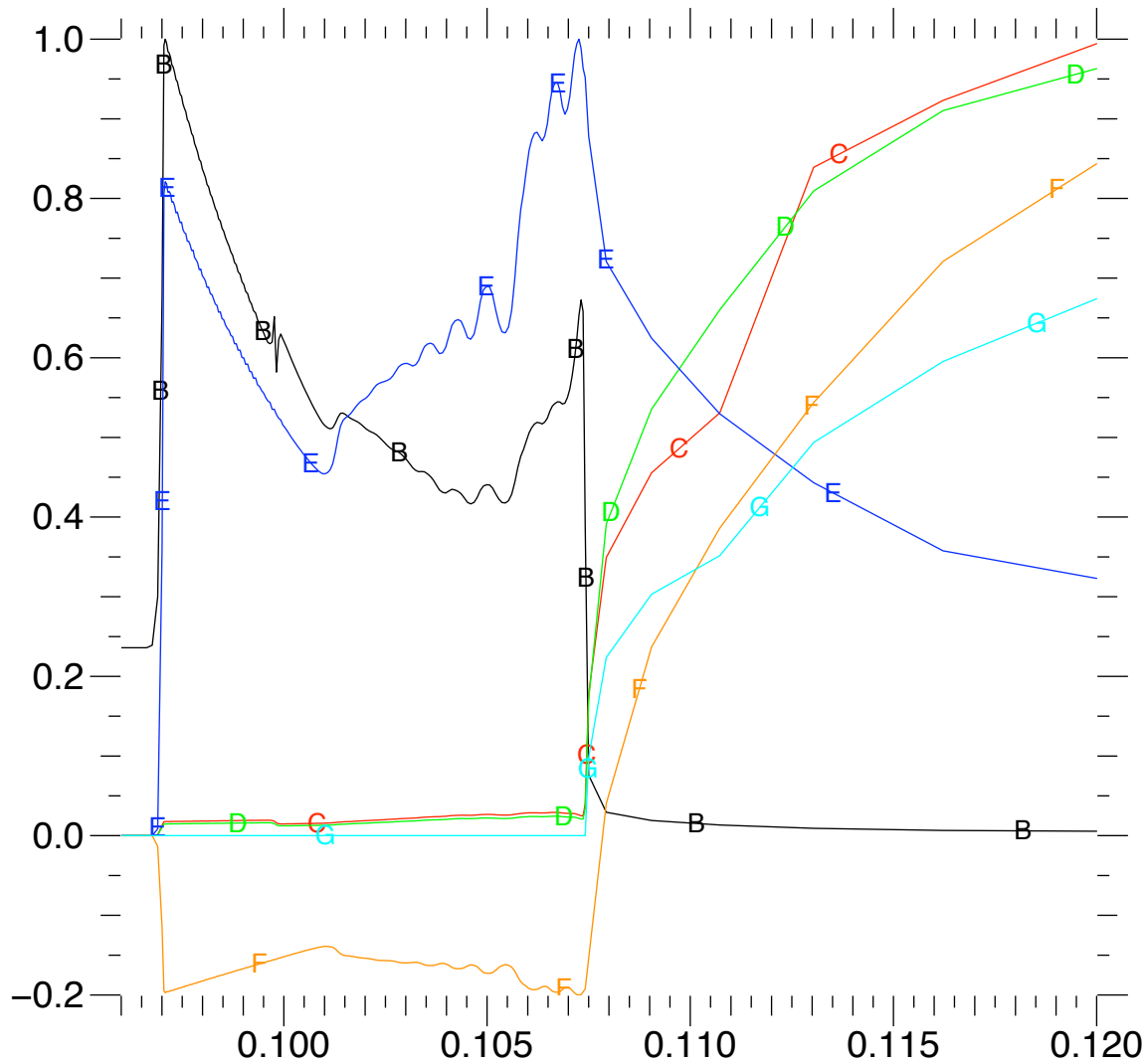
B: plg, density/max(density), r
C: plg, ion_temp/max(ion_temp), r
D: plg, electron_temp/max(electron_temp), r
E: plg, pressure/max(pressure), r
F: plg, -0.2*velocity/min(velocity), r
G: plg, integral_laser_deposition/max(integral_laser_deposition), r

```
radial slice at         0.250000 nanoseconds
max density          =          4.26179 g/cc
max ion temp         =          481.348 eV
max electron temp    =          826.913 eV
max total pressure   =          25.6320 Mb
max inward velocity  =      -7.66044e+06 cm/sec
total laser deposition per unit volume * dV =          6.80198 TW
```
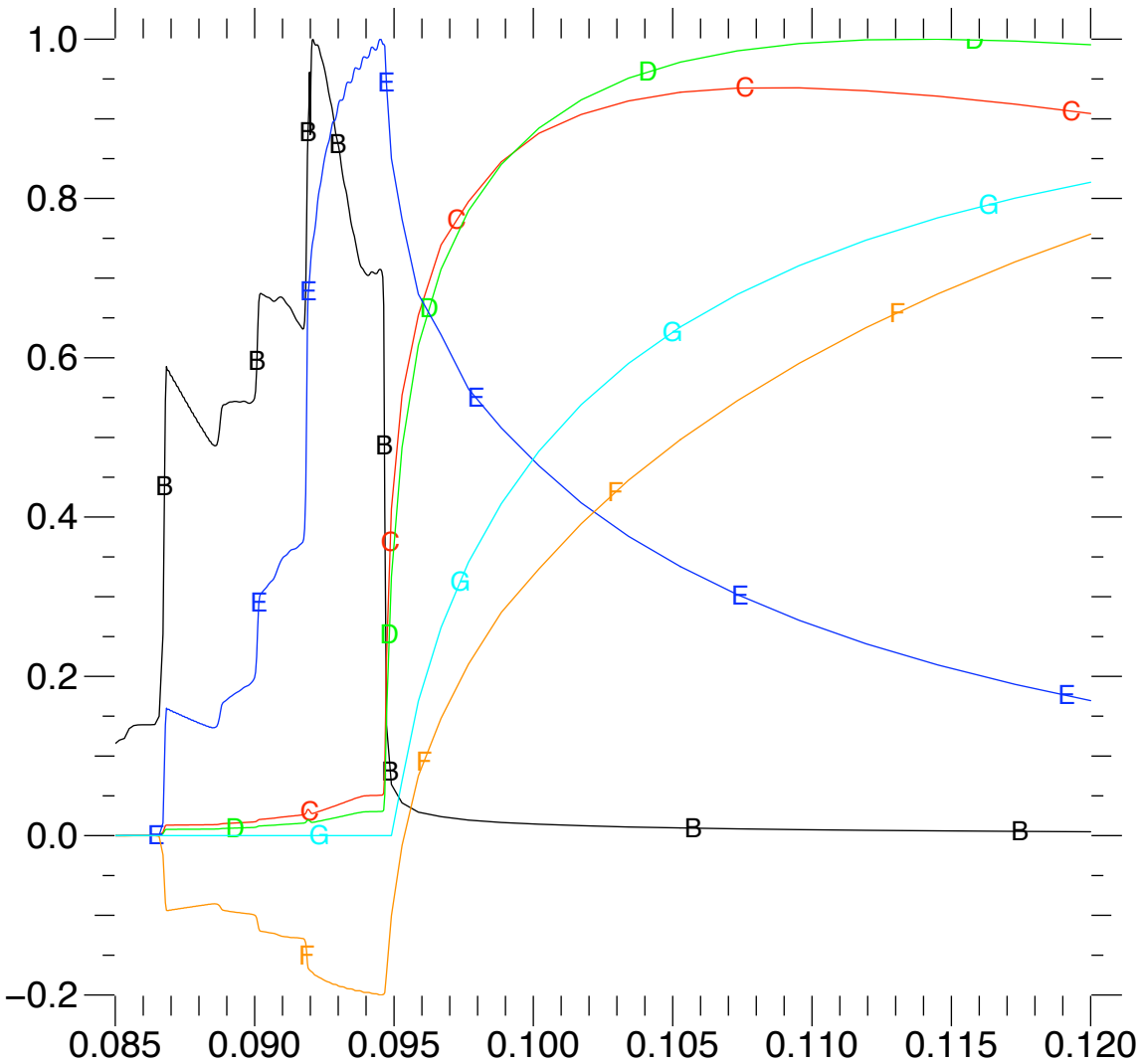
B: plg, density/max(density), r
C: plg, ion_temp/max(ion_temp), r
D: plg, electron_temp/max(electron_temp), r
E: plg, pressure/max(pressure), r
F: plg, -0.2*velocity/min(velocity), r
G: plg, integral_laser_deposition/max(integral_laser_deposition), r

radial slice at   3.00000 nanoseconds
max density   =   1.08656 g/cc
max ion temp   =   534.478 eV
max electron temp   =   639.698 eV
max total pressure   =   7.39039 Mb
max inward velocity   =   -4.33583e+06 cm/sec
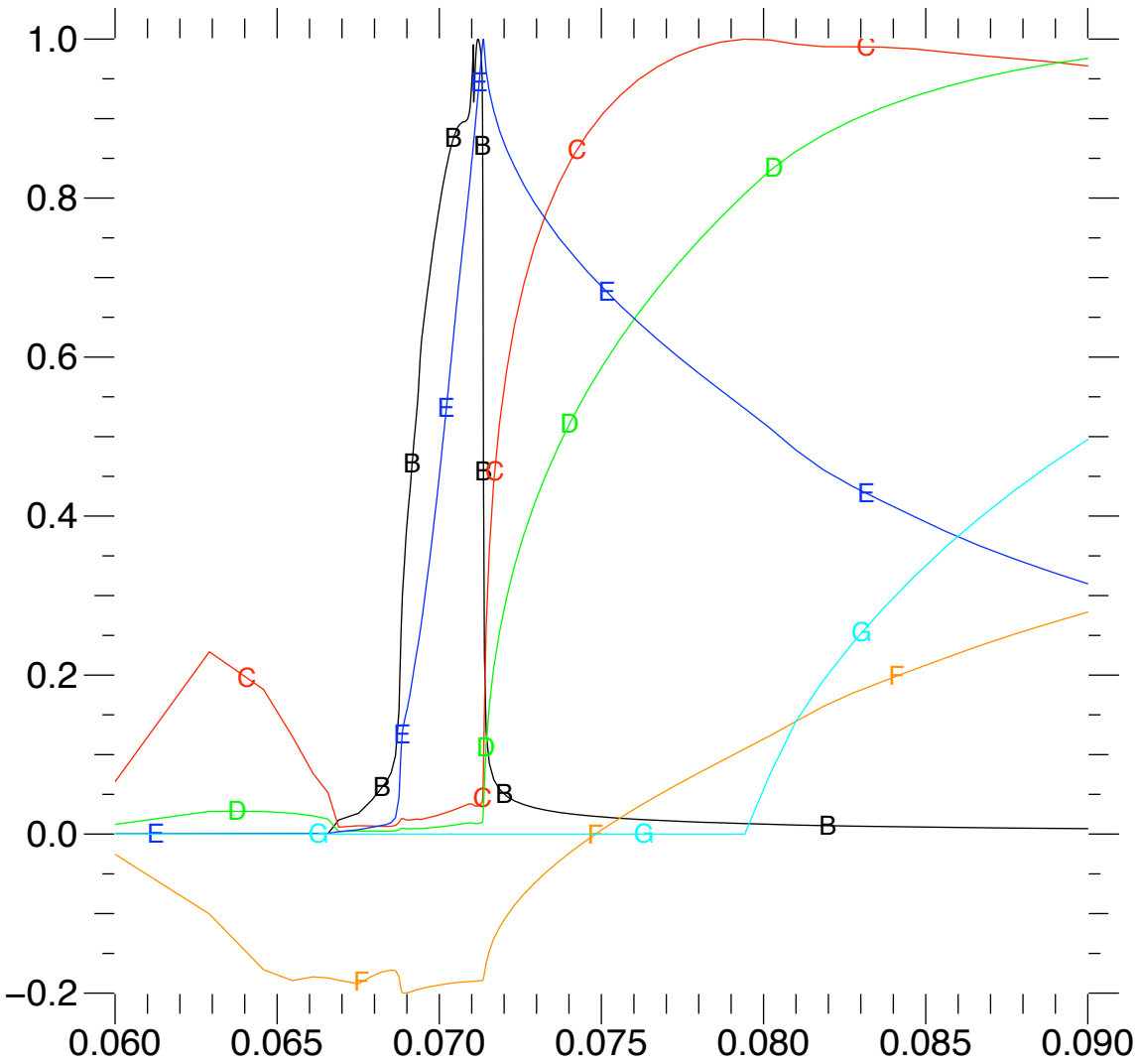total laser deposition per unit volume * dV =   1.44856 TW

```
filename = ftst
creation date = 2007−10−10 14:26:11
print date = Fri Dec  7 07:45:35 2007
```

B: plg, density/max(density), r
C: plg, ion_temp/max(ion_temp), r
D: plg, electron_temp/max(electron_temp), r
E: plg, pressure/max(pressure), r
F: plg, −0.2*velocity/min(velocity), r
G: plg, integral_laser_deposition/max(integral_laser_deposition), r

```
radial slice at          5.00000 nanoseconds
max density         =          1.84051 g/cc
max ion temp        =          536.782 eV
max electron temp   =          896.189 eV
max total pressure  =          27.8106 Mb
max inward velocity =     −7.73655e+06 cm/sec
total laser deposition per unit volume * dV =          5.51530 TW
```
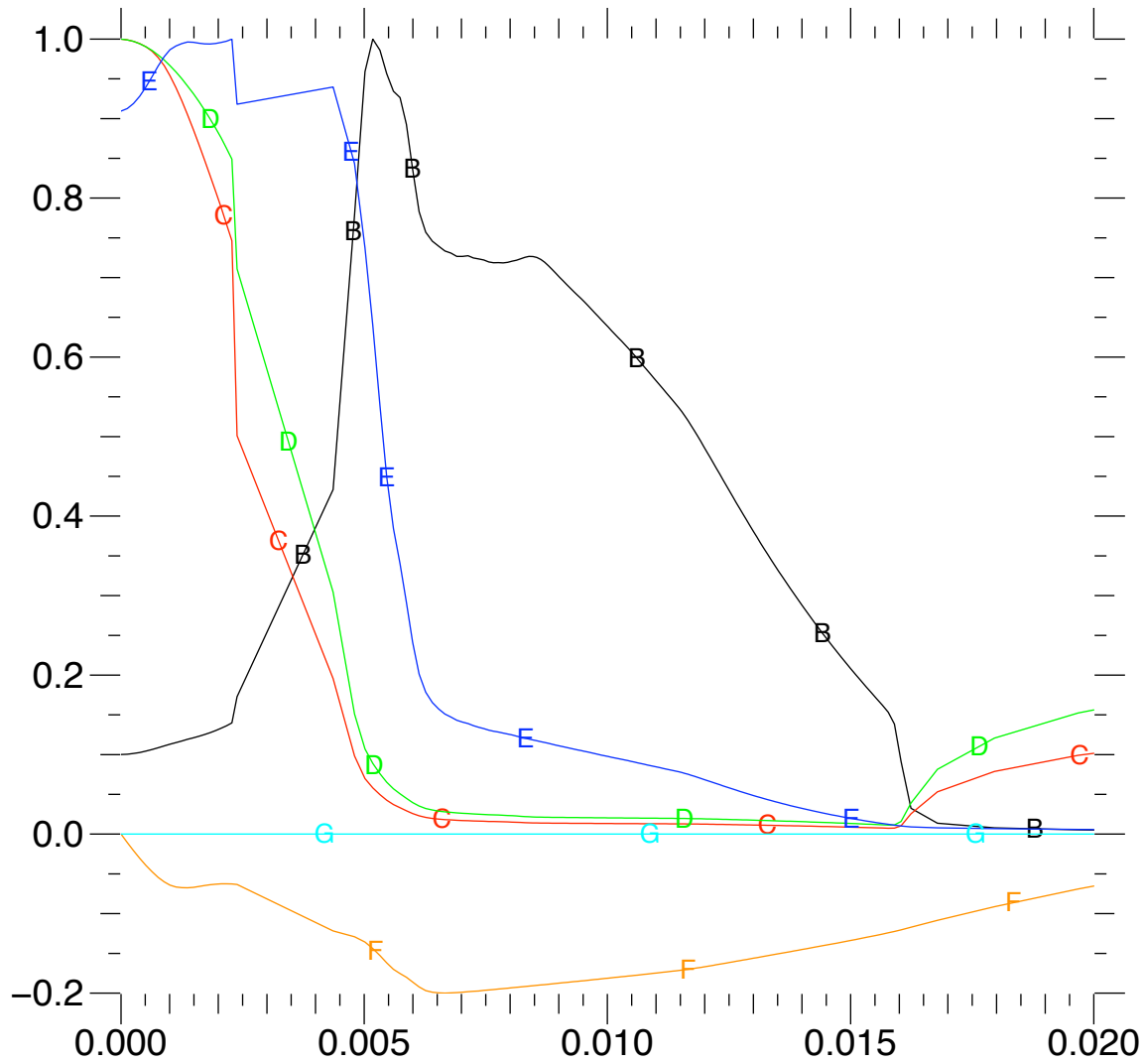
B: plg, density/max(density), r
C: plg, ion_temp/max(ion_temp), r
D: plg, electron_temp/max(electron_temp), r
E: plg, pressure/max(pressure), r
F: plg, -0.2*velocity/min(velocity), r
G: plg, integral_laser_deposition/max(integral_laser_deposition), r

radial slice at   6.80000 nanoseconds
max density   =   5.86687 g/cc
max ion temp   =   971.216 eV
max electron temp   =   2596.03 eV
max total pressure   =   173.268 Mb
max inward velocity   =   -2.35617e+07 cm/sec
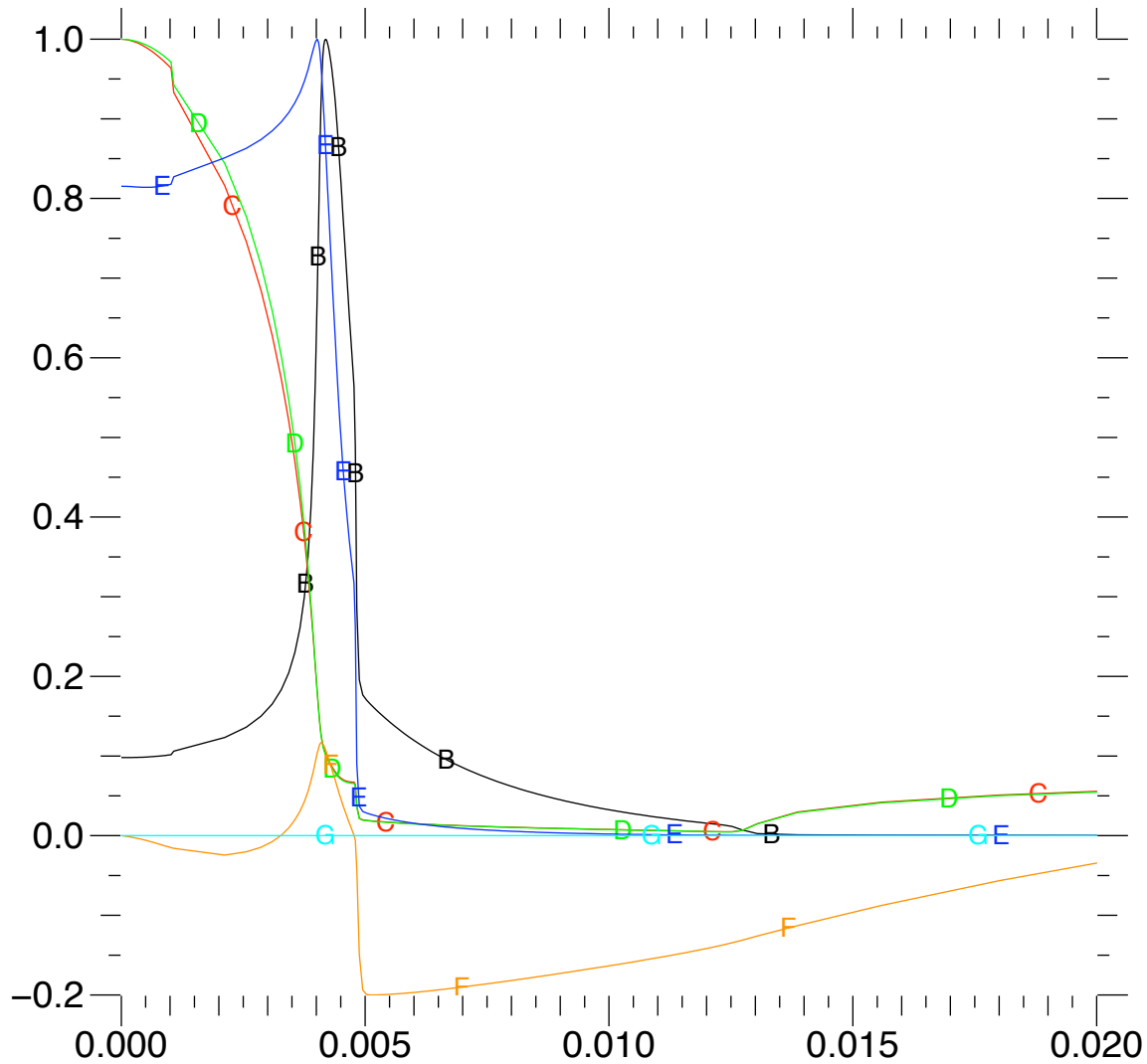total laser deposition per unit volume * dV =   40.9039 TW

B: plg, density/max(density), r
C: plg, ion_temp/max(ion_temp), r
D: plg, electron_temp/max(electron_temp), r
E: plg, pressure/max(pressure), r
F: plg, -0.2*velocity/min(velocity), r
G: plg, integral_laser_deposition/max(integral_laser_deposition), r

radial slice at   8.56000 nanoseconds
max density   =   71.5057 g/cc
max ion temp   =   7743.99 eV
max electron temp   =   5059.23 eV
max total pressure =   38005.3 Mb
max inward velocity =   -4.57143e+07 cm/sec
total laser deposition per unit volume * dV =   7.85318e-32 TW

filename = ftst
creation date = 2007-10-10 14:26:11
print date = Fri Dec 7 07:49:09 2007

B: plg, density/max(density), r
C: plg, ion_temp/max(ion_temp), r
D: plg, electron_temp/max(electron_temp), r
E: plg, pressure/max(pressure), r
F: plg, -0.2*velocity/min(velocity), r
G: plg, integral_laser_deposition/max(integral_laser_deposition), r

radial slice at   8.69000 nanoseconds
max density   =   923.143 g/cc
max ion temp   =   13547.3 eV
max electron temp   =   13838.1 eV
max total pressure   =   1.14796e+06 Mb
max inward velocity =   -3.54046e+07 cm/sec
total laser deposition per unit volume * dV =   7.85319e-32 TW